https://doi.org/10.5194/egusphere-2025-1354
Preprint. Discussion started: 31 March 2025

The tracer nudging method for correcting and preventing uneven tracer distributions in geodynamical models

Paul J. Tackley[1]

[1]Department of Earth and Planetary Sciences, ETH Zurich, Zurich, 8092, Switzerland

Correspondence to: Paul J. Tackley (ptackley@ethz.ch)

Abstract. Tracers/markers/particles are commonly used in geodynamical models to track composition and sometimes temperature throughout the domain. A common problem is that over time, gaps in the tracer distribution can develop, often resulting in cells with no tracers as well as bunching of tracers. Here a correction method that perturbs or "nudges" the positions of tracers in such a way as to close gaps and eliminate bunching is presented. Test results show that this tracer nudging method is highly effective. Starting from an extremely heterogeneous tracer distribution with large regions of the domain devoid of tracers, it can produce an even distribution in only a few nudge iterations. In a time-stepping situation with a nudge every time-step, the amplitudes of the nudges are small yet sufficient to prevent gaps and bunches, allowing a low-order tracer advection method to be used while maintaining a tracer distribution that is more even than that obtained using higher-order advection methods alone. The nudge essentially corrects any non-conservation error inherent in an advection method. The computational cost is small because the method simply requires solving a Poisson equation.

1 Introduction

Tracers, alternatively named markers or particles, are commonly used in geodynamical models to track composition and sometimes temperature, typically in the framework of a so-called "marker-and-cell" or "particle-in-cell" method, in which velocity and pressure are calculated on a fixed Eulerian grid while various other quantities are advected on Lagrangian tracers/markers/particles (e.g. (Harlow and Welch, 1965; Tackley and King, 2003; Gerya and Yuen, 2007)). All of the major geodynamical modelling codes include this option, including CitcomS (Moresi et al., 2014), Aspect (Heister et al., 2017), Stag3D/StagYY (Tackley and King, 2003; Tackley, 2008), TERRA (e.g. Panton et al., 2025), LaMEM (Kaus et al., 2016), and I3ELVIS (Gerya et al., 2015).

This method relies on many tracers (e.g. 5-50) being present in each cell. Thus, it is problematic that over time, gaps in the tracer distribution typically develop, often resulting in cells containing no tracers. At the same time, bunching of tracers builds up. Such gaps and bunches may develop due to inaccuracies in tracer advection methods or modelling complex processes such as eruption or intrusion of molten tracers with associated compaction of the melt source region (e.g. Lourenco et al., 2020). The development of such gaps and bunches can be minimized by an optimal choice of tracer advection method (Pusok et al., 2016; Gerya et al., 2021) but apparently not eliminated, particularly since geodynamical simulations spanning

https://doi.org/10.5194/egusphere-2025-1354
Preprint. Discussion started: 31 March 2025

the age of the Earth may require millions of time steps, giving small inaccuracies plenty of time to build up. Thus, some remedy is required. One remedy is to create new tracers to fill the gaps (Gerya, 2019).

Another remedy, presented here, is to perturb or "nudge" the positions of tracers in such a way as to close gaps and eliminate bunching. If performed frequently such as every time step, the amplitudes of the nudges are small yet sufficient to prevent large-scale gaps and bunches from building up. In this usage, the method corrects any non-conservation (in the sense of not being divergence-free everywhere) inherent in the method used to advect tracers. The method also works well when starting from an extremely uneven tracer distribution with large fractions of the domain initially devoid of tracers.

Irregularities in the spatial distribution of tracers can be quantified in terms of the number of tracers per unit area, typically calculated on a cell-by-cell basis. If tracers are considered to each have a mass (equal to the total mass of the domain divided by the number of tracers), then this can alternatively be thought of as a density, i.e. mass of tracers per unit area. Thus, the goal of this method is to nudge tracer positions in order to achieve a constant tracer density throughout the model domain.

In subsequent sections the mathematical theory is presented, followed by various tests of its effectiveness using the accompanying MATLAB program in two and three dimensions. This method has already been implemented and is in regular use in the geodynamical modelling code StagYY (Tackley, 2008).

2 Mathematical Theory

As the goal is to achieve a constant tracer density, the first step is to calculate the current tracer density $\rho_t(x,y,z)$, defined as the mass (or number) of tracers per unit volume and calculated on a cell-by-cell basis. It is important that ρ_t changes smoothly as tracers move around, which it does not if one simply counts the number of tracers in each cell, because a tracer crossing a cell boundary causes an abrupt change in the densities of the two cells. Therefore, linear averaging of tracers to cells is important – termed "shape function" averaging by Tackley and King (2003) and widely recommended (e.g. Gerya, 2019; Ismail-Zadeh and Tackley, 2013). In this, each tracer contributes to the mass in 4 (in 2-D) or 8 (in 3-D) cells, linearly dependent on its distance from the cell centres using bilinear (in 2-D) or trilinear (in 3-D) functions analogous to the shape functions used in the finite element method. Once the tracer-based density in each cell is known, the tracer density error can then be calculated as

$$\Delta\rho_e = \rho_t - \rho_c \ , \qquad (1)$$

where ρ_c is the correct density (e.g. of rock). This can in general vary with position, but for the purposes of the tests in this paper is assumed to be constant.

The required perturbation ("nudging") of tracer positions can be derived starting with the equation expressing conservation of mass:

https://doi.org/10.5194/egusphere-2025-1354
Preprint. Discussion started: 31 March 2025

$$\frac{\partial \rho}{\partial t} = -\nabla \cdot (\rho \vec{v}) \,, \tag{2}$$

where ρ is the density field, $\vec{v}$ is the velocity field and t is time. Multiplying (2) by a finite time interval leads to an approximate equation relating a finite change in density to a finite perturbation in position $\Delta\vec{x}$, which is here applied to the tracer density ρ_t:

$$\Delta\rho_t \approx -\nabla \cdot (\rho_t \Delta\vec{x}) \,. \tag{3}$$

$\Delta\vec{x}$ can conveniently be expressed as the gradient of a displacement potential ϕ:

$$\Delta\vec{x} = \frac{\nabla\phi}{\rho_t} \,. \tag{4}$$

Substituting (4) into (3) leads to a Poisson equation for ϕ:

$$\Delta\rho_t = -\nabla^2\phi \,. \tag{5}$$

The desired change in density $\Delta\rho_t$ is minus the density error, $\Delta\rho_e$, therefore the equation to solve is

$$\nabla^2\phi = \Delta\rho_e \,. \tag{6}$$

This can easily and efficiently be solved using standard methods such as multigrid. Assuming that the domain boundaries are impermeable, the appropriate boundary condition for ϕ is zero gradient perpendicular to the boundary.

It is noted that another possible expression for $\Delta\vec{x}$ is

$$\Delta\vec{x} = \nabla\phi \tag{7}$$

leading to

$$\Delta\rho_t = \nabla \cdot (\rho_t \nabla\phi) \,, \tag{8}$$

which is slightly more difficult to solve and problematic in areas where $\rho_t = 0$, if such areas exist. Equation (4) also seems problematic in areas where $\rho_t = 0$ but as there are no tracers in these areas, there is no problem in practice.

This method does not achieve a perfectly uniform tracer distribution in a single nudge because ρ_t changes (towards the correct density ρ_c) during the displacement of tracers: equation (2) is an approximation. In areas of too-high ρ_t (decreasing during the correction step), equation (4) underpredicts the displacement, whereas in areas of too-low ρ_t (increasing during the correction step), equation (4) overpredicts the displacement. Thus, when calculating the displacement from equation (4) it is best to use an average of the initial density and the correct density, rather than only the initial density. Tests indicate that a geometric average gives slightly better convergence than an arithmetic average, but both perform considerably better than using just the starting ρ_t. In summary, when calculating displacement, equation (4) is replaced by:

$$\Delta\vec{x} = \frac{\nabla\phi}{\sqrt{(\rho_t \rho_c)}} \,. \tag{9}$$

https://doi.org/10.5194/egusphere-2025-1354
Preprint. Discussion started: 31 March 2025

A single application of this algorithm achieves a considerable reduction of the density error (quantified using the L1 or L2 norm), which is sufficient during a time-stepping situation. If, however, starting from an extremely non-uniform tracer distribution with large portions of the domain being devoid of tracers, several iterations of the algorithm may be needed, as documented in Section 4.

3 Accompanying MATLAB scripts

This method is implemented in two and three dimensions in the accompanying MATLAB scripts (Tackley and ETH Zurich, 2025) (main program NUDGE.m), which can run the various test cases documented and discussed in Section 4. MATLAB scripts have the advantage of being easy to translate into other science and engineering-oriented high-level languages that include multi-dimensional arrays and array algebra, such as Julia (Bezanson, 2017) or modern Fortran (Metcalf et al., 2024). Indeed, the method has already been implemented in the Fortran geodynamical modelling code StagYY (Tackley, 2008) and is in regular use.

The accompanying program uses a multigrid solver to obtain the displacement potential field. This is highly efficient but does require that the number of cells be a power-of-2 in each direction, or a power-of-2 times a small integer. Resolution is set by the number of cells in each direction *nx, ny and nz*, and the number of tracers by *tracers_per_cell*. Two-dimensional cases can be run by setting the number of y-points *ny=1*. Densities are calculated at cell centres, while displacements and velocities are defined at cell boundaries in the standard staggered-grid finite volume arrangement (e.g. Harlow and Welch 1965; Patankar, 1980) as used by many codes in the geodynamical modelling community (e.g. Ogawa et al., 1991; Tackley, 1993; Trompert and Hansen, 1996; Gerya and Yuen, 2007; Kameyama et al. 2008; Tackley, 2008; Kaus et al., 2016). Domain boundaries are coincident with the perpendicular displacement/velocity points. Tracer positions are initialised either on a regular grid (with a smaller grid spacing than that on which the velocities/displacements are calculated), on a regular grid with random perturbations of up to half a grid spacing, or completely randomly. Initialising tracers on a regular grid causes artefacts with tracer alignment when they are advected, so regular + random is optimal. Completely random positions cause a density error that is typically a factor of 2 larger than regular + random, as shown later. The domain depth is assumed to be 1.0 and the grid spacing is the same in all three physical directions, meaning that the domain width in the x and y directions is given by (nx/nz) and (ny/nz), respectively.

The MATLAB m-files are:

- NUDGE.m: The main program that runs and plots individual tests or test suites.
- correct_tracer_density.m: Performs the "nudging" algorithm detailed in Section 2.
- tracer_density.m: Calculates the cell-based tracer density field.
- Poisson_solve.m: Solves Poisson equation in 2-D or 3-D assuming zero-gradient boundary conditions.
- advect_tracers.m: Performs 1st-order Euler, 2nd-order or 4th-order Runge-Kutta tracer advection.

The core of the nudging algorithm in correct_tracer_density.m is compact, consisting of only four lines (Fig. 1).

https://doi.org/10.5194/egusphere-2025-1354
Preprint. Discussion started: 31 March 2025


```
dens  = tracer_density(tra,nx,ny,nz);          % calculate tracer density
phi   = Poisson_solve (dens-mean(dens,"all")); % calculate displacement potential
displ = displacement  (phi,dens);              % calculate displacement field
tra   = advect_tracers(tra,displ,1,true,L);    % nudge tracers
```

Figure 1. MATLAB implementation of the algorithm in Section 2, in file correct_tracer_density.m

4 Tests

The first set of tests starts with various extremely non-uniform tracer distributions and tests how rapidly (in terms of number of nudging iterations) the method can create a uniform tracer distribution. Then follows a time-stepping test, using a simple analytically defined flow field and low order advection method.

4.1 Highly non-uniform tracer distribution tests

Various idealized initial tracer distributions are tested:

(i) Half-empty. Half of the domain is empty of tracers.
(ii) Rectangular hole. A rectangular region in the middle of the domain is empty of tracers.
(iii) Spherical hole. A spherical region in the centre of the domain is empty of tracers.
(iv) Sphere. All tracers are in a sphere in the centre of the domain, the rest being empty.
(v) Random. Tracers are placed randomly in the entire domain.

Figure 2 (top row) shows these initial conditions and Fig. 2 (rows 2-5) shows the results of the first four correction nudges. After two nudges (a "nudge-nudge"; Fig. 2 middle row) tracers fill the domain; the subsequent nudge-nudge evens them out further. The evenness of the tracer distribution is quantified by tracer density plots in Fig. 3. After one nudge-nudge there is still significant unevenness, but this becomes difficult to discern after a further nudge-nudge. Random initial tracer positions (right column) lead to substantial initial unevenness in tracer density.

Figure 4 shows how the L1 norm of tracer density error decreases with number of nudges for the 2-D tests (Figs. 2 and 3) and for 3-D versions of the tests. For highly non-uniform initial conditions the reduction in tracer density error is more than an order of magnitude after 2 nudges, then becomes less rapid. Again, the random initial condition has substantial tracer density error approaching 0.2. 3-D cases are similar but with slightly slower convergence for the "sphere" case.

A problem in initial tests of the “sphere” case was that many tracers were nudged through the domain boundaries. This is due to the extreme nature of this test and is not a problem in a normal time-stepping application, but nevertheless a solution has been found. An approach that does not work is to place these tracers at the closest point inside the domain, although this does work for normal tracer advection by a velocity field that does not cross the boundaries. However, in this application the displacement field can substantially cross the boundaries, leading to a build-up of tracers at the boundaries, tracers that are not easily nudged away from there (close to the boundaries the perpendicular displacement is 0). What does work is to detect tracers that are nudged beyond external boundaries and instead apply only a fraction of the displacement to them. A fraction of 70% was found to be optimal.

https://doi.org/10.5194/egusphere-2025-1354
Preprint. Discussion started: 31 March 2025

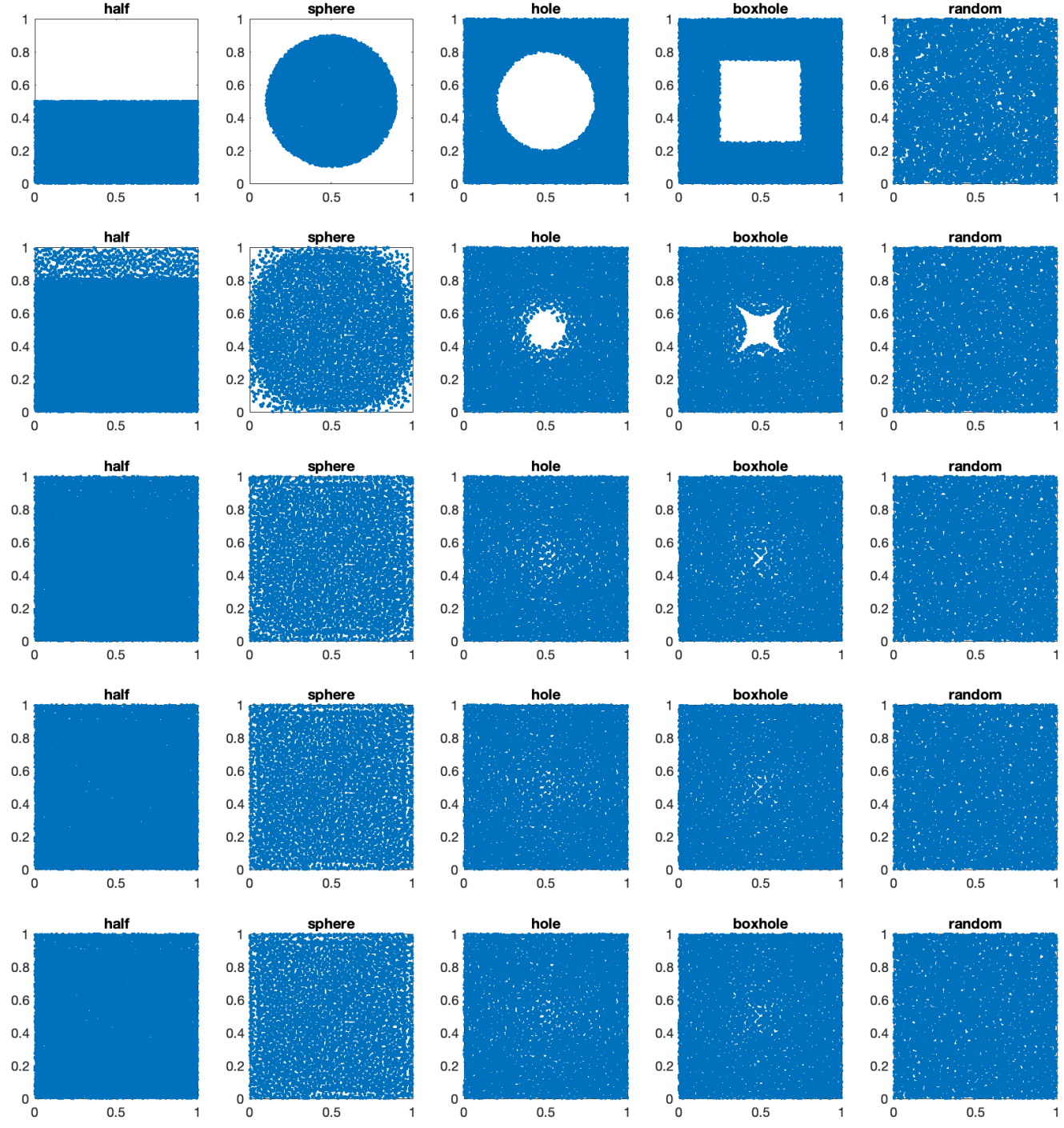

Figure 2. Tracer positions in the five highly nonuniform tests performed in 2-D with 32x32 cells and 10 tracers per cell on average. Each column is one test case. Shown are (top row) the initial condition and (rows 2 - 5) nudges 1-4.

https://doi.org/10.5194/egusphere-2025-1354
Preprint. Discussion started: 31 March 2025

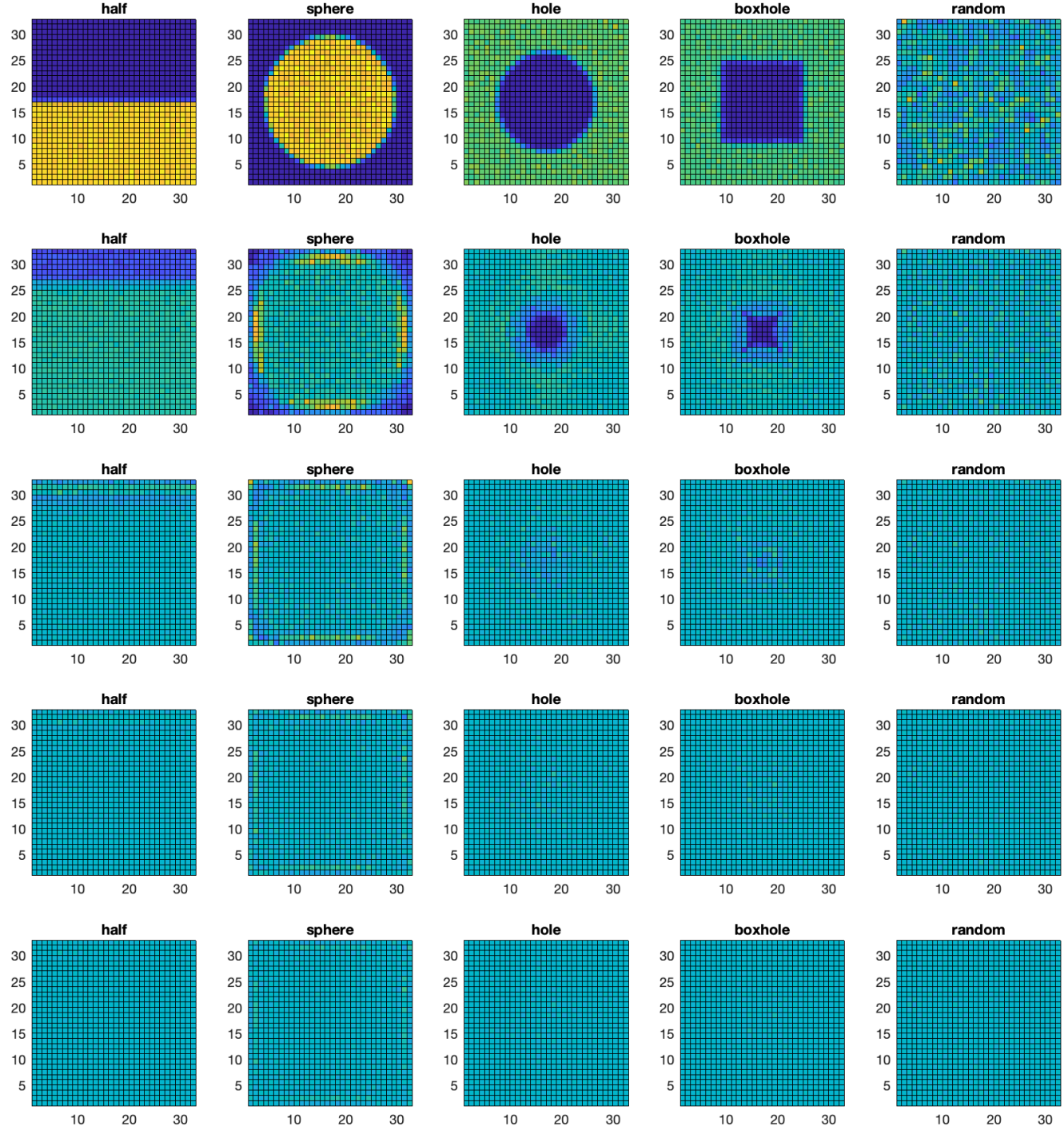

155 **Figure 3. Tracer density error fields for the tracer distributions shown in Figure 2. The colour scale is the same for all frames.**

https://doi.org/10.5194/egusphere-2025-1354
Preprint. Discussion started: 31 March 2025

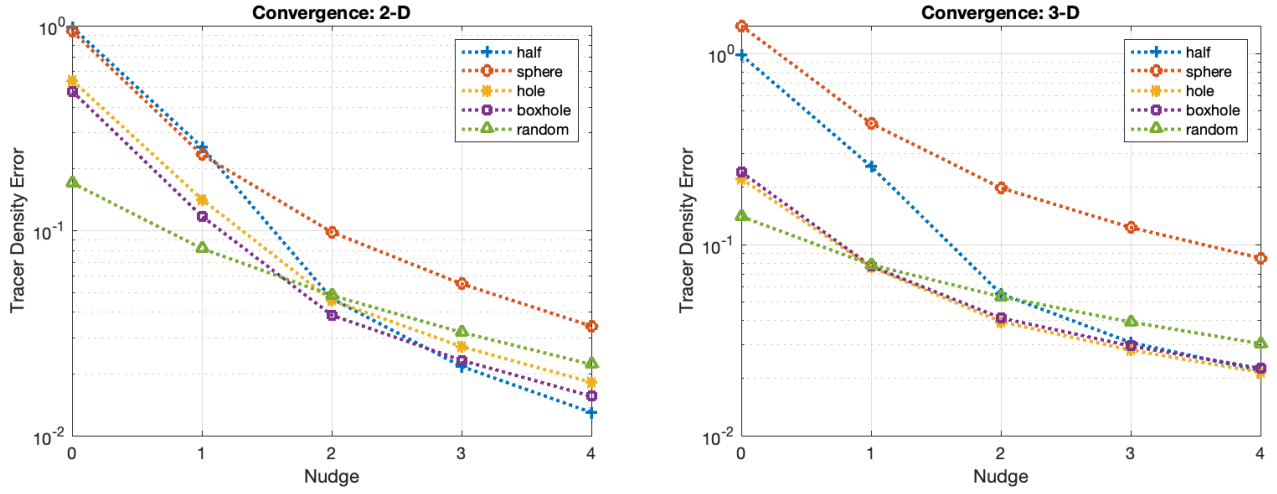

Figure 4. L1 norm of tracer density error versus number of nudges for the 5 initial tracer distributions in (left) 2-D 32x32 cells and (right) 3-D 32x32x32 cells, in both cases with 10 tracers per cell on average.

4.2 Time-stepping test

The goal in this test is to determine whether the tracer nudging method can prevent gaps and bunches from building up in a time-stepping situation, as this is what is typically used in geodynamical simulations. Tracers are advected according to an analytically defined velocity field given by the curl of a two-dimensional stream function S(x,z):

$$v_x = \frac{dS}{dz} \quad v_y = 0 \quad v_z = -\frac{dS}{dx} \quad . \tag{10}$$

The resulting flow field is divergence-free for any S. In the presented tests, S is defined by

$$S(x,z) = \frac{1}{\pi} sin\left(\pi \frac{x}{L_x}\right) sin\left(\pi \frac{z}{L_z}\right) \tag{11}$$

where L_x is the length of the domain in the x-direction and L_z is the length of the domain in the z-direction. This gives a one-cell circulation pattern with no flow through the boundaries and velocities given by:

$$v_x = sin\left(\pi \frac{x}{L_x}\right) cos\left(\pi \frac{z}{L_z}\right) \qquad v_z = -\frac{1}{L_x} cos\left(\pi \frac{x}{L_x}\right) sin\left(\pi \frac{z}{L_z}\right) \tag{12}$$

In order to maximize the challenge of maintaining a uniform tracer distribution, tracers are advected using the first order forward Euler method, which usually makes them spiral outwards and concentrate towards the outside of the domain. Additionally, they are initialized in completely random positions. This combination (Euler+nudge+random) is compared to three advection methods without any nudging: Euler, 2nd-oder Runge-Kutta and 4th-order Runge-Kutta methods with tracers

https://doi.org/10.5194/egusphere-2025-1354
Preprint. Discussion started: 31 March 2025

initialized on a (regular+random) grid. Velocities at the staggered grid points are calculated using the expressions above and linearly interpolated to tracer positions.

Figure 5 shows tracer distributions and density error fields after 100 time-steps of nondimensional time 0.05 on a 32x32 grid with an average of 10 tracers per cell. As the maximum velocity given by equation (12) is 1, tracers move a maximum distance of 0.05 in one step. As expected, the Euler method (2nd column) is quite inaccurate, with tracers spiraling outwards and building up towards the domain boundaries and corners. With the addition of a single nudge per step (left column), however, the tracer distribution remains even and negligible tracer density error is visible. The 2nd- and 4th-order Runge-Kutta methods produce similar results to each other, with significant unevenness visible in the tracer density error field.

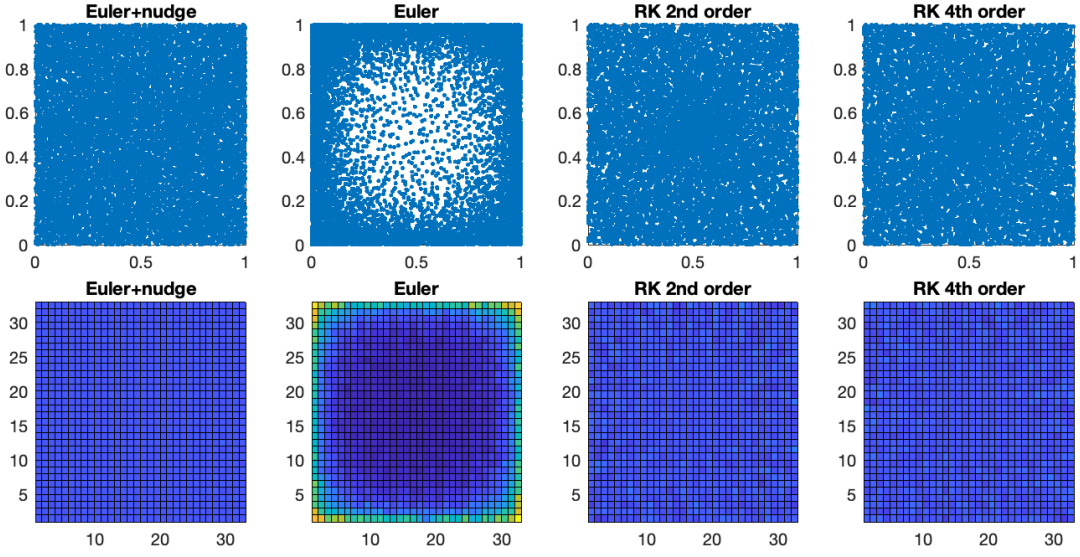

Figure 5. Tracer distributions (top row) and associated density error fields (bottom row) for the 4 advection methods on a 32x32 grid with an average of 10 tracers per cell.

The time-evolution of tracer density error is quantified in Fig. 6, which shows the L1-norm versus time step. At the initial condition (step 0) there is more than a factor of 2 higher density error in the "Euler + nudge" case than the other cases because tracer positions are completely random, whereas in the other cases tracers are initialized on a regular grid with random perturbations. This indicates that the latter initial condition is much better. Subsequently, the "Euler" case rapidly develops a large density error, whereas adding a single nudge per step causes a reduction of density error to a low value, which is subsequently maintained. In both Runge-Kutta cases the error increases steadily from the initial condition, surprisingly at a similar rate for the 2nd- and 4th-order schemes.

https://doi.org/10.5194/egusphere-2025-1354
Preprint. Discussion started: 31 March 2025

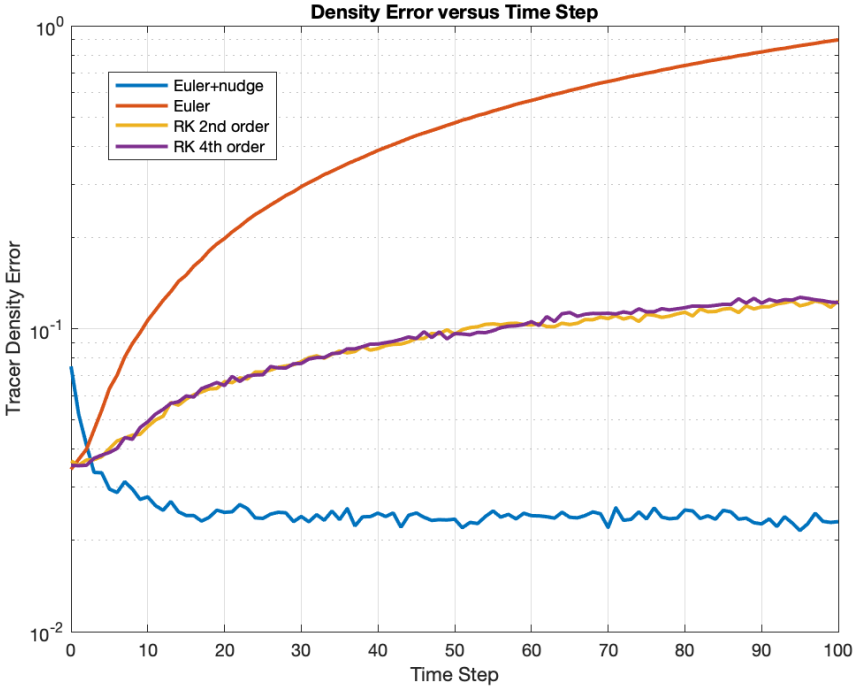

Figure 6. L1-norm of tracer density error versus time step for the tests in Figure 5.

5. Conclusions

The tracer nudging method is an effective way of eliminating and preventing gaps and bunching of tracers in geodynamical models/simulations. Starting from an extremely heterogeneous distribution with large regions of the domain devoid of tracers, it can produce an even distribution in only a few nudge iterations. In a time-stepping situation it allows a low-order tracer advection method to be used while maintaining a tracer distribution that is more even than that obtained using high-order advection methods alone. Essentially, the nudge corrects any non-conservation error inherent in an advection method. The computational cost is small because it simply involves solving a Poisson equation, which is much faster than the Stokes solve that has to be performed every time step (multiple times for non-linear rheology).

Code availability. The exact version of the MATLAB code used to produce the results and figures used in this paper is archived on Zenodo under the MIT license under DOI 10.5281/zenodo.15065274 (Tackley and ETH Zurich, 2025). No input data or additional scripts are required.

Competing interests. The author declares that he has no conflict of interest.

Special issue statement. Advances in numerical modelling of geological processes

https://doi.org/10.5194/egusphere-2025-1354
Preprint. Discussion started: 31 March 2025

Acknowledgments. The author is grateful to ETH Zurich. The author was motivated to write this method up by discussions on tracer advection with Boris Kaus, Thibault Duretz and Taras Gerya.

References

Bezanson, J., Edelman, A., Karpinski, S. and Shah, V. B: Julia: A fresh approach to numerical computing, SIAM Review, 59, 65-98, doi: 10.1137/141000671, 2017.

Gerya, T.V.: Introduction to Numerical Geodynamic Modelling (2nd Edition), Cambridge University Press, Cambridge, UK, https://doi.org/10.1017/9781316534243, 2019.

Gerya, T., Duretz, T., and Räss, L.: New continuity-based velocity interpolation scheme for staggered grids, EGU General Assembly 2021, online, 19–30 Apr 2021, EGU21-15308, https://doi.org/10.5194/egusphere-egu21-15308, 2021.

Gerya, T. V., Stern, R. J., Baes, M., Sobolev, S. V. and Whattam, S. A.: Plate tectonics on the Earth triggered by plume-induced subduction initiation, Nature, 527, 221–225, doi:10.1038/nature15752, 2015.

Gerya, T.V. and Yuen, D.A.: Robust characteristics method for modelling multiphase visco-elasto-plastic thermo-mechanical problems, Physics of the Earth and Planetary Interiors, 163, 83-105, doi:10.1016/j.pepi.2007.04.015, 2007.

Harlow, F.H. and Welch, J.E.: Numerical calculation of time-dependent viscous incompressible flow of fluid with free surface, Phys. Fluids A, 8, 2182-2189, doi:10.1063/1.1761178, 1965.

Heister, T., Dannberg, J., Gassmöller, J. and Bangerth, W.: High Accuracy Mantle Convection Simulation through Modern Numerical Methods – II: Realistic Models and Problems, Geophysical Journal International, 210 (2), 833–851, doi:10.1093/gji/ggx195, 2017

Ismail-Zadeh, A. and Tackley, P.J.: Computational Methods for Geodynamics, Cambridge University Press, Cambridge, UK, doi:10.1017/CBO9780511780820, 2010.

Kameyama, M., Kageyama, A. and Sato, T.: Multigrid-based simulation code for mantle convection in spherical shell using yin-yang grid, Phys. Earth Planet. Int., 171, 19-32, doi:10.1016/j.pepi.2008.06.025, 2008.

Kaus, B. J. P., Popov, A. A., Baumann, T. S., Püsök, A. E., Bauville, A., Fernandez, N. and Collignon, M.: Forward and inverse modelling of lithospheric deformation on geological timescales, NIC Series, 48, ISBN 978-3-95806-109-5, pp. 299, http://hdl.handle.net/2128/9842, 2016.

Lourenço, D. L., Rozel, A. B., Ballmer, M. D. and Tackley, P. J.: Plutonic-Squishy Lid: A New Global Tectonic Regime Generated by Intrusive Magmatism on Earth-Like Planets, Geochemistry, Geophysics, Geosystems, 21, doi:10.1029/2019gc008756, 2020.

Metcalf, M., Reid, J., Cohen, M. and Bader, R.: Modern Fortran Explained, Incorporating Fortran 2023, Oxford University Press, 576 Pages, ISBN: 9780198876588, 2024.

https://doi.org/10.5194/egusphere-2025-1354
Preprint. Discussion started: 31 March 2025

Moresi, L., Zhong, S., Han, L., Conrad, C., Tan, E., Gurnis, M., Choi, E., Thoutireddy, P., Manea, V., McNamara, A., Becker, T., Leng, W., and Armendariz, L..: CitcomS v3.3.1 (v3.3.1), Zenodo. https://doi.org/10.5281/zenodo.7271920, 2014.

Ogawa, M., Schubert, G. and Zebib, A.: Numerical simulations of 3-dimensional thermal convection in a fluid with strongly temperature-dependent viscosity, J. Fluid Mech., 233, 299-328, doi:10.1017/S0022112091000496, 1991.

Panton, J., Davies, J. H., Koelemeijer, P., Myhill, R. and Ritsema J.: Unique composition and evolutionary histories of large low velocity provinces, *Sci Rep*, *15*(1), 4466, doi:10.1038/s41598-025-88931-3, 2025.

Patankar, S.V.: Numerical Heat Transfer and Fluid Flow, CRC Press, doi:10.1201/9781482234213, 1980.

Pusok, A.E., Kaus, B.J.P. and Popov, A.A.: On the Quality of Velocity Interpolation Schemes for Marker-in-Cell Method and Staggered Grids, Pure and Applied Geophysics, 174, 1071-1089, doi:10.1007/s00024-016-1431-8, 2016.

Tackley, P.J.: Effects of strongly temperature-dependent viscosity on time-dependent, 3-dimensional models of mantle convection, Geophys. Res. Lett., 20, 2187-2190, doi:10.1029/93GL02317, 1993.

Tackley, P.J.: Modelling compressible mantle convection with large viscosity contrasts in a three-dimensional spherical shell using the yin-yang grid, Phys. Earth Planet. Int., doi:10.1016/j.pepi.2008.1008.1005, 2008.

Tackley, P.J. and ETH Zurich: Software accompanying manuscript "The tracer nudging method for correcting and preventing uneven tracer distributions in geodynamical models" (1.0), Zenodo. https://doi.org/10.5281/zenodo.15065274, 2025.

Tackley, P.J. and King, S.D.: Testing the tracer ratio method for modeling active compositional fields in mantle convection simulations, Geochem. Geophys. Geosyst., 4, doi:10.1029/2001GC000214, 2003.

Trompert, R.A. and Hansen, U.: The application of a finite-volume multigrid method to 3-dimensional flow problems in a highly viscous fluid with a variable viscosity, Geophys. Astrophys. Fluid Dyn., 83, 261-291, doi:10.1080/03091929608208968, 1996.